Paramagnetic enhancement of nuclear spin-spin coupling

Peter John Cherry,[†] Syed Awais Rouf,[‡] and Juha Vaara[*,‡]

Institute of Inorganic Chemistry, Slovak Academy of Sciences, Dúbravská cesta 9, SK-84536 Bratislava, Slovakia, and NMR Research Unit, P.O. Box 3000, FIN-90014 University of Oulu, Finland

E-mail: juha.vaara@iki.fi

Abstract

We present a derivation and computations of the paramagnetic enhancement of the nuclear magnetic resonance (NMR) spin-spin coupling, which may be expressed in terms of the hyperfine coupling (HFC) and (for systems with multiple unpaired electrons) zero-field splitting (ZFS) tensors. This enhancement is formally analogous to the hyperfine contributions to the NMR shielding tensor as formulated by Kurland and McGarvey. The significance of the spin-spin coupling enhancement is demonstrated by using a combination of density-functional theory and correlated *ab initio* calculations, to determine the HFC and ZFS tensors, respectively, for two paramagnetic 3d metallocenes, a $Cr(II)(acac)_2$ complex, a Co(II) pyrazolylborate complex, and a lanthanide system, Gd-DOTA. Particular attention is paid to relativistic effects in HFC tensors, which are calculated using two methods: a nonrelativistic method supplemented by perturbational spin-orbit coupling corrections, and a fully relativistic, 4-component matrix-Dirac-Kohn-Sham approach. The paramagnetic enhancement lacks a direct dependence on the

---

[*]To whom correspondence should be addressed
[†]Institute of Inorganic Chemistry, Slovak Academy of Sciences, Dúbravská cesta 9, SK-84536 Bratislava, Slovakia
[‡]NMR Research Unit, P.O. Box 3000, FIN-90014 University of Oulu, Finland

distance between the coupled nuclei, and represents more the strength and orientation of the individual hyperfine couplings of the two nuclei to the spin density distribution. Therefore, the enhancement gains relative importance as compared to conventional coupling as the distance between the nuclei increases, or generally in the cases where the conventional coupling mechanisms result in a small value. With the development of the experimental techniques of paramagnetic NMR, the more significant enhancements, *e.g.*, of the $^{13}C^{13}C$ couplings in the Gd-DOTA complex (as large as 9.4 Hz), may eventually become important.

Introduction

Spin-spin coupling constants (SSCCs) have long been used in nuclear magnetic resonance (NMR) for determination of the structure of electronically closed-shell, diamagnetic molecules.[1] Unfortunately, SSCCs are rarely measured for open-shell, paramagnetic systems; the fast nuclear relaxation and associated spectral broadening make it difficult to obtain information about the interaction of the moments of nuclei close to the paramagnetic center.[2] As the experimental techniques of paramagnetic NMR (pNMR) improve,[3] more SSCCs for paramagnetic systems will become experimentally accessible, necessitating development of a theoretical framework for the description of these couplings. A key step towards developing such a theory is to acquire an understanding of how paramagnetic phenomena, such as hyperfine coupling (HFC) and zero-field splitting (ZFS, in systems with more than one unpaired electron), can impact the SSC tensors.

The lack of precise information regarding SSCCs for paramagnetic systems means that they are usually approximated with SSCCs obtained from corresponding diamagnetic systems.[4,5] This approach is common in the determination of the NMR constraints used in structural calculations,[6] and the results of numerous publications attest to the validity of this approximation.[7,8] A reason for this success is that the nuclei experiencing strong paramagnetic effects reside near the paramagnetic center, whereas, in contrast, nuclei that are far from the center are relatively unaffected by paramagnetic phenomena. Hence, the SSCCs of these distant nuclei resemble those in corresponding diamagnetic systems. The strong interactions near the paramagnetic center cause rapid

relaxation, resulting in a pNMR "blind" zone, from which signals cannot be obtained.[9] There-fore, it is usually the nuclei that are far from the paramagnetic center that are focused upon in contemporary pNMR investigations.

Recent developments in ultrafast magic-angle spinning have enabled, *e.g.*, the determination of the contributions to the pseudocontact shift of nuclei close to the paramagnetic center.[3] Theoretical work has shown how paramagnetic phenomena — HFC, the electronic Zeeman interaction param-eterized by the *g*-tensor, and ZFS — cause substantial paramagnetic modification of the NMR chemical shifts of the nuclei in this region. Furthermore, current investigations indicate that even seemingly small variations in the geometry near the paramagnetic center can have a significant impact on the NMR shifts of ligands on the outer limits of the complex.[10] This suggests that ac-curate description of the structure near the paramagnetic center is becoming increasingly topical. Accordingly, it would be useful to have a tool for assessing the magnitude of the paramagnetic modification of the SSC tensors for nuclei that are (1) at a sufficient distance from the param-agnetic center to feature resolvable *J*-couplings and (2) still influenced by paramagnetic effects. Anticipating experimental developments in the determination of SSCCs also close to the paramag-netic center, similar to those seen for the chemical shift, we have in this work derived theoretical expressions for the paramagnetic enhancement of the SSC tensors.

Following the procedure established in Ref.[12] and described later (e.g., in Ref.[13]), this paper develops expressions for describing how the nuclear spin-spin coupling term in the NMR spin Hamiltonian is modified by paramagnetic effects at each of the two coupled nuclei. This method is then applied to two 3*d* metallocenes (nickelocene and chromocene), a Cr(II) acetyl-acetatonate complex, a larger Co(II) structure, as well as a lanthanide compound. To provide an indication of the relative significance of this effect, the enhancements calculated for the two paramagnetic metallocenes are compared to the (unenhanced) SSCCs of the diamagnetic ferrocene. Our cen-tral Eq. (6) for the enhancement was already put forward by Autschbach[11] by analogy with the hyperfine pNMR shielding contribution.

The results presented in this paper suggest that, in coordination complexes with large ZFS and

HFC, which also give rise to a large paramagnetic chemical shift contribution, the SSC enhancement is sufficiently large to be relevant to the analysis of experimental pNMR data. Interestingly, unlike in the case of normal SSCCs, the paramagnetic enhancement is shown not to have a direct dependence on the distance between the two nuclei. As a result, the paramagnetic enhancement of the SSCCs between nuclei at large internuclear separation or, *e.g.*, geminal couplings, can potentially be much larger than the coupling between similar nuclei in analogous diamagnetic molecules.

Theory

Kurland-McGarvey spin-spin coupling theory

In Ref.,[13] the Kurland-McGarvey theory[12] for the NMR shielding tensor of nuclei in paramagnetic molecules was reviewed in the special case of a ground-state multiplet characterized by a ZFS Hamiltonian of the form $\hat{H}_{\mathrm{ZFS}} = \mathbf{S} \cdot \mathbf{D} \cdot \mathbf{S}$, where $\mathbf{S}$ is the effective spin operator. Within the assumption of a relatively weak spin-orbit (SO) coupling[14,15] the paramagnetic enhancement of shielding and chemical shift may be determined from the HFC tensors of the nuclei in question, the $\mathbf{D}$ matrix parameterizing ZFS, and the *g*-tensor of the system. In this article, the procedure of Kurland and McGarvey is used to derive an analogous expression for the paramagnetic enhancement of the SSC tensor. The resulting formula requires calculation of only the ZFS tensor and the HFC tensors for the relevant nuclei.

We present the detailed derivation of the SSC enhancement tensor, $\mathbf{J}^p_{KL}$, in the Supporting Information (SI), where the following expression is obtained for the Cartesian $\varepsilon\tau$ component

$$J^p_{KL,\varepsilon\tau} = -\frac{1}{hkT} \frac{\sum_{nm} Q_{nm} \langle n|\hat{h}^{\mathrm{hf}}_{K,\varepsilon}|m\rangle \langle m|\hat{h}^{\mathrm{hf}}_{L,\tau}|n\rangle}{\sum_q \exp\left(\frac{-E_q}{kT}\right)}. \tag{1}$$

Here, the matrix $\mathbf{Q}$ is defined [12,13] as

$$Q_{nm} = \begin{cases} \exp\left(\frac{-E_n}{kT}\right) & \text{if } E_n = E_m \\ \\ -\frac{\left[\exp\left(\frac{-E_m}{kT}\right) - \exp\left(\frac{-E_n}{kT}\right)\right]kT}{E_m - E_n} & \text{if } E_n \neq E_m \end{cases} \tag{2}$$

in terms of the eigenvalues and -states, E_n and $|n\rangle$, of the nuclear spin-independent part of the molecular Hamiltonian, $\hat{H}^{(0)}$. This matrix encodes the thermal populations of $|n\rangle$. There are magnetic couplings between the states [13] via the hyperfine operator $\hat{\mathbf{h}}^{\text{hf}}$, defined for nucleus K (with spin vector $\mathbf{I}_K$) as

$$\hat{H}_K^{\text{hf}} = \sum_\varepsilon \hat{h}_{K,\varepsilon}^{\text{hf}} I_{K,\varepsilon}. \tag{3}$$

Expression (1) can be rewritten by defining the hyperfine operator in terms of the HFC part of the effective electron paramagnetic resonance (EPR) spin Hamiltonian,

$$H_{\text{EPR}}^{\text{hf}} = \sum_K \mathbf{S} \cdot \mathbf{A}_K \cdot \mathbf{I}_K. \tag{4}$$

Here, $\mathbf{A}_K$ is the HFC tensor and we may, then, identify

$$\hat{h}_{K,\varepsilon}^{\text{hf}} = \sum_a S_a A_{K,a\varepsilon}. \tag{5}$$

This redefinition of the hyperfine operator in terms of the HFC tensor of EPR represents a transition from a full description that would make use of all the states of the unperturbed molecular Hamiltonian, to a very limited version of perturbation theory, which only makes use of the states within the lowest multiplet. Hence, the summation in Eq. (1) is effectively truncated to only include the eigenstates of the Hamiltonian $\hat{H}^{(0)} = \mathbf{S} \cdot \mathbf{D} \cdot \mathbf{S}$. This is valid provided that the energy gap between the lowest multiplet and the excited multiplets is large, as this renders the denominator of relevant components of Q_{nm} large.

5

Using this approximation, the tensor components of the paramagnetic SSC enhancement may be rewritten as

$$J^p_{KL,\varepsilon\tau} = -\frac{1}{hkT}\sum_{ab}A_{K,a\varepsilon}\langle S_aS_b\rangle A_{L,b\tau},$$

(6)

where

$$\langle S_aS_b\rangle = \sum_{nm}Q_{nm}\frac{\langle n|S_a|m\rangle\langle m|S_b|n\rangle}{\sum_q\exp\left(\frac{-E_q}{kT}\right)}.$$

(7)

Dyadic $\langle \mathbf{SS}\rangle$

Expression (6) is identical to the Kurland-McGarvey formula for the pNMR shielding tensor, save the change in the prefactor and the replacement of the g-tensor with the HFC tensor of the second coupled nucleus. In particular, the dyadic $\langle S_aS_b\rangle$ that describes how the spin density distribution of the system mediates the effects of the hyperfine interactions between the two coupled nuclei, is identical to that in the shielding theory.[12,13] This dyadic is roughly analogous to the suscep-tibility tensor,[4,10] where the spin density constitutes the polarizable medium. It is worth noting that, at temperatures sufficiently high to render the zero-field split states of the ground multiplet equally populated, the trace of $\langle S_aS_b\rangle$ is equal to $S(S+1)$.[13] Therefore, there is an important con-nection, besides strong HFC at the nuclei, between high spin multiplicity and large paramagnetic enhancement.

To gain insight into the nature of the enhancement we consider the case of a doublet (*i.e.*, $\langle S^2\rangle = \frac{3}{4}, S_z = \frac{1}{2}$), devoid of ZFS, for which the $\langle S_aS_b\rangle$ dyadic can be written as

$$\langle \mathbf{SS}\rangle = \frac{1}{3}S(S+1)\begin{bmatrix}1 & 0 & 0\\ 0 & 1 & 0\\ 0 & 0 & 1\end{bmatrix} = \begin{bmatrix}\frac{1}{4} & 0 & 0\\ 0 & \frac{1}{4} & 0\\ 0 & 0 & \frac{1}{4}\end{bmatrix}.$$

(8)

In this case the coupling of the HFC tensors of the two nuclei by the spin density [in Eq. (6)] occurs via a completely isotropic $\langle \mathbf{SS}\rangle$ matrix. This reflects the fact that, in the absence of ZFS (or with ZFS but at sufficiently high temperature[13]), all relative directions in which the coupled spins are

located, are equivalent in energy. When the response of the spin density is isotropic, there only remains an implicit dependence of the paramagnetic SSC enhancement on the vector connecting the two coupled nuclei. This dependence is contained in the HFC tensors $\mathbf{A}_K$ and $\mathbf{A}_L$ of the nuclei. Hence, the position of the coupled nuclei relative to one another is only significant in the sense that it affects the product $\mathbf{A}_K \cdot \mathbf{A}_L$. In the case of doublet spin multiplicity, or in the doublet-like, high-temperature limit of higher-multiplicity systems,[13] $\langle \mathbf{SS} \rangle$ is completely isotropic [see Eq. (8)], and its eigenvalues are equal.

In situations where neither of the above criteria are fulfilled, not all orientations of the coupled nuclei with respect to the unpaired spin distribution are equivalent, however. Then, the paramagnetic SSC enhancement encodes information about the relative direction of the vectors from the paramagnetic center to the two coupled nuclei. Therefore, in addition to spin multiplicity and the magnitude of HFC affecting the size of the coupling enhancement, the orientation of the principal axes of the HFC tensors relative to the principal axes of the $\langle \mathbf{SS} \rangle$ dyadic, must also be taken into account.

Contributions to paramagnetic enhancement

The paramagnetic SSC enhancement results from a combination of a number of different physical effects. Starting from the perspective of the nonrelativistic (NR) HFC tensor, corrected perturbationally for SO coupling,[13,16] a break-down to the different physical contributions to the HFC can be presented as:

$$\mathbf{A}_K = A_K^{\mathrm{con}} \mathbf{1} + \mathbf{A}_K^{\mathrm{dip}} + A_K^{\mathrm{pc}} \mathbf{1} + \mathbf{A}_K^{\mathrm{dip},2} + \mathbf{A}_K^{\mathrm{as}}. \tag{9}$$

Here, $\mathbf{1}$ is the 3×3 identity matrix, whereas A_K^{con} and $\mathbf{A}_K^{\mathrm{dip}}$ are the isotropic Fermi contact and anisotropic dipolar coupling respectively. In addition to these large NR contributions, there are the following, smaller terms: A_K^{pc}, the isotropic (tensorial rank 0), so-called pseudocontact coupling, $\mathbf{A}_K^{\mathrm{dip},2}$, the anisotropic and symmetric (rank-2) "second dipolar term", and $\mathbf{A}_K^{\mathrm{as}}$, the anisotropic and antisymmetric (rank-1) term. The last three terms arise from the relativistic SO corrections

7

to the HFC (see Ref.[17] and references therein). The two NR terms are of the second order in the fine structure constant α, whilst the three relativistic terms are of the order $\mathscr{O}(\alpha^4)$. This expansion of $\mathbf{A}_K$ can be substituted into Eq. (6), to obtain the different physical contributions to the paramagnetic enhancement of $\mathbf{J}_{KL}$ (see Table 1). The decomposition of $\mathbf{A}_K$ in Eq. (9) is specific to the case where SO coupling has been applied to $\mathbf{A}_K$ as a perturbative correction and scalar relativistic effects are omitted.[13,16] This approach can in principle be motivated in the normal pNMR context, when studying the interaction of light nuclei in a heavy-atom compound. However, significant scalar relativistic effects have been pointed out in studies of pNMR shielding tensors for transition element systems.[18,19] In this article, the perturbational description of SO effects in HFC is contrasted with a fully relativistic 4-component method,[20] in which both SO coupling and scalar relativistic effects are included variationally in the optimization of the wavefunction. This is expected to provide a better description of relativistic influences, particularly in the cases where one or both of the coupled nuclei reside close to the heavy nucleus. In the 4-component calculations, $\mathbf{J}^p$ is presently decomposed into only three terms: J^p_{con}, $\mathbf{J}^p_{\mathrm{dip}}$, and $\mathbf{J}^p_{\mathrm{con-dip}}$.

Table 1: Contributions to paramagnetic enhancement, $\mathbf{J}^p_{KL}$, of the spin-spin coupling tensor $\mathbf{J}_{KL}$.

Term in $J^p_{KL,\varepsilon\tau}$	Expression in Eq. (6)	Order[a]	Rank[b]
J^p_{con}	$A^{\mathrm{con}}_K A^{\mathrm{con}}_L \langle S_\varepsilon S_\tau \rangle$	$\mathscr{O}(\alpha^4)$	0,2
$J^p_{\mathrm{con-dip}}$	$A^{\mathrm{con}}_K \sum_b \langle S_\varepsilon S_b \rangle A^{\mathrm{dip}}_{L,b\tau} + A^{\mathrm{con}}_L \sum_a A^{\mathrm{dip}}_{K,a\varepsilon} \langle S_a S_\tau \rangle$	$\mathscr{O}(\alpha^4)$	0,2,1
J^p_{dip}	$\sum_{ab} A^{\mathrm{dip}}_{K,a\varepsilon} \langle S_a S_b \rangle A^{\mathrm{dip}}_{L,b\tau}$	$\mathscr{O}(\alpha^4)$	0,2,1
$J^p_{\mathrm{con-pc}}$	$(A^{\mathrm{con}}_K A^{\mathrm{pc}}_L + A^{\mathrm{con}}_L A^{\mathrm{pc}}_K) \langle S_\varepsilon S_\tau \rangle$	$\mathscr{O}(\alpha^6)$	0,2
$J^p_{\mathrm{con-dip2}}$	$A^{\mathrm{con}}_K \sum_b \langle S_\varepsilon S_b \rangle A^{\mathrm{dip,2}}_{L,b\tau} + A^{\mathrm{con}}_L \sum_a A^{\mathrm{dip,2}}_{K,a\varepsilon} \langle S_a S_\tau \rangle$	$\mathscr{O}(\alpha^6)$	0,2,1
$J^p_{\mathrm{con-as}}$	$A^{\mathrm{con}}_K \sum_b \langle S_\varepsilon S_b \rangle A^{\mathrm{as}}_{L,b\tau} + A^{\mathrm{con}}_L \sum_a A^{\mathrm{as}}_{K,a\varepsilon} \langle S_a S_\tau \rangle$	$\mathscr{O}(\alpha^6)$	2,1
$J^p_{\mathrm{dip-pc}}$	$A^{\mathrm{pc}}_K \sum_b \langle S_\varepsilon S_b \rangle A^{\mathrm{dip}}_{L,b\tau} + A^{\mathrm{pc}}_L \sum_a A^{\mathrm{dip}}_{K,a\varepsilon} \langle S_a S_\tau \rangle$	$\mathscr{O}(\alpha^6)$	0,2,1
$J^p_{\mathrm{dip-dip2}}$	$\sum_{a,b} (A^{\mathrm{dip}}_{K,a\varepsilon} A^{\mathrm{dip,2}}_{L,b\tau} + A^{\mathrm{dip,2}}_{K,a\varepsilon} A^{\mathrm{dip}}_{L,b\tau}) \langle S_a S_b \rangle$	$\mathscr{O}(\alpha^6)$	0,2,1
$J^p_{\mathrm{dip-as}}$	$\sum_{a,b} (A^{\mathrm{dip}}_{K,a\varepsilon} A^{\mathrm{as}}_{L,b\tau} + A^{\mathrm{as}}_{K,a\varepsilon} A^{\mathrm{dip}}_{L,b\tau}) \langle S_a S_b \rangle$	$\mathscr{O}(\alpha^6)$	0,2,1

[a] The order of the fine structure constant, which indicates the relative significance of each contribution. [b] The tensorial ranks of $\mathbf{J}^p_{KL}$ that the term contributes to. All terms of order $\mathscr{O}(\alpha^8)$ and higher have been omitted; such terms would be comparatively small as $\alpha \approx 1/137$. The leading terms in the normal diamagnetic spin-spin coupling tensor appear in $\mathscr{O}(\alpha^4)$.

Computational Details

Calculations were performed on the paramagnetic ($S = 1$) metallocenes $NiCp_2$ (nickelocene) and $CrCp_2$ (chromocene), diamagnetic $FeCp_2$ (ferrocene), on a larger Co(III) pyrazolylborate complex (HPYBCO, a $S = \frac{3}{2}$ system studied in Ref. [21]), as well as $S = \frac{3}{2}$ $Cr(acac)_2$. The structures for these molecules were optimized in the TURBOMOLE software[22] using density-functional theory (DFT) with the B3LYP[23] exchange-correlation functional, which includes 20% Hartree-Fock exchange. For the metallocenes, the def2-TZVP[24] basis set was used with the eclipsed geometry, as described in Ref. [13] In the case of HPYBCO, the def2-TZVP basis set was only used on the light atoms, whilst a Stuttgart-type energy-consistent, scalar-relativistic effective core potential ECP10MDF (with ten electrons in the core)[25] and the appropriate $8s7p6d2f1g/6s5p3d2f1g$ (in the primitive/contracted notation) valence basis set[26] were used for the Co(II) center (see Ref. [21] for more information). The optimized geometries for $NiCp_2$ and $CrCp_2$ can be found in Ref. [13] and those for HPYBCO in Ref. [21] The coordinates of $FeCp_2$ are deposited in the SI. Furthermore, the $Cr(acac)_2$ complex was investigated, with geometry optimized in ORCA[27] also using the B3LYP functional with Grimme's D3 dispersion correction[28] and a TZVPP basis.[29] The coordinates of $Cr(acac)_2$ can be found in the SI.

ZFS tensors were calculated using the complete-active space self-consistent field (CASSCF) method followed by N-electron valence-state perturbation theory (NEVPT2)[30] using the ORCA program and a DKH-TZVP basis.[31] The active spaces used for the state-averaged, scalar relativistic (second-order Douglas-Kroll-Hess[32,33]) CASSCF calculations were (8,5) for $NiCp_2$, (4,5) for $CrCp_2$, (7,5) for HPYBCO, and (4,5) for $Cr(acac)_2$, where the standard (number of electrons, number of orbitals in active space) format is used. In all these cases the active space consisted of the five d-type atomic orbitals on the metal center, and the maximum number of possible orthogonal roots with the S, $(S-1)$ and $(S+1)$ spin quantum numbers was used in each case. These calculations used locally dense basis sets,[34] consisting of the DKH-TZVP basis on the metal ion and the atoms bonded directly to it, and the DKH-SVP[31] basis on the more distant atoms. The performance of such locally dense basis sets has been shown to be reliable for calculations of ZFS

and the *g*-tensor in the context of pNMR chemical shifts.[13,21] For the metallocenes and $Cr(acac)_2$ the TZVP-quality basis was used for all atoms.

The calculation of the ZFS tensor for Gd-DOTA followed the same procedure as the HPYBCO calculations, with three exceptions: The active space was (7,7), with the seven f-electrons of the Gd ion correlated, the DKH-TZVP basis was used for all the atoms, and the geometry was adopted from Ref.[35]

The HFC tensors were calculated by unrestricted DFT using both ORCA and RESPECT-MDKS[36] codes. In ORCA, the PBE0 exchange-correlation functional[37,38] and the full def2-TZVP basis set on all atoms, were employed. RESPECT-MDKS is a fully relativistic matrix-Dirac-Kohn-Sham program, and it was used with the same functional but with an entirely decontracted version of the DKH-TZVP basis. The $\mathbf{J}_{\mathrm{iso}}^p$ obtained using the fully relativistic HFCs were compared to the results obtained with HFCs corrected for perturbational SO interaction effects only, obtained using ORCA.

For the closed-shell $FeCp_2$ molecule, the conventional diamagnetic CC, CH, and HH SSCCs were calculated, to put the isotropic paramagnetic enhancement, J_{iso}^p, in contrast. These calculations were performed in GAUSSIAN 09,[39] using the def2-TZVP basis for the carbon and hydrogen atoms, as well as the ECP10MDF pseudopotential and the corresponding valence basis for the Fe atom.

Results and discussion

Metallocene complexes

To determine the significance of the paramagnetic enhancement proposed here, we can compare the computed isotropic rotational average of $\mathbf{J}^p$ for the paramagnetic metallocenes, $NiCp_2$ and $CrCp_2$, to the "unenhanced", standard SSCCs in an analogous diamagnetic system ($FeCp_2$). Approximating the SSCCs for a paramagnetic molecule with those for the corresponding diamagnetic molecule is sometimes performed in spin dynamics simulations.[8] However, if the paramagnetic

enhancement is large, this approximation is not valid. While it is possible to experimentally determine SSCCs for nuclei in paramagnetic molecules, the broad NMR lines often render the precision of the measurements low, particularly for nuclei near the paramagnetic center.[5]
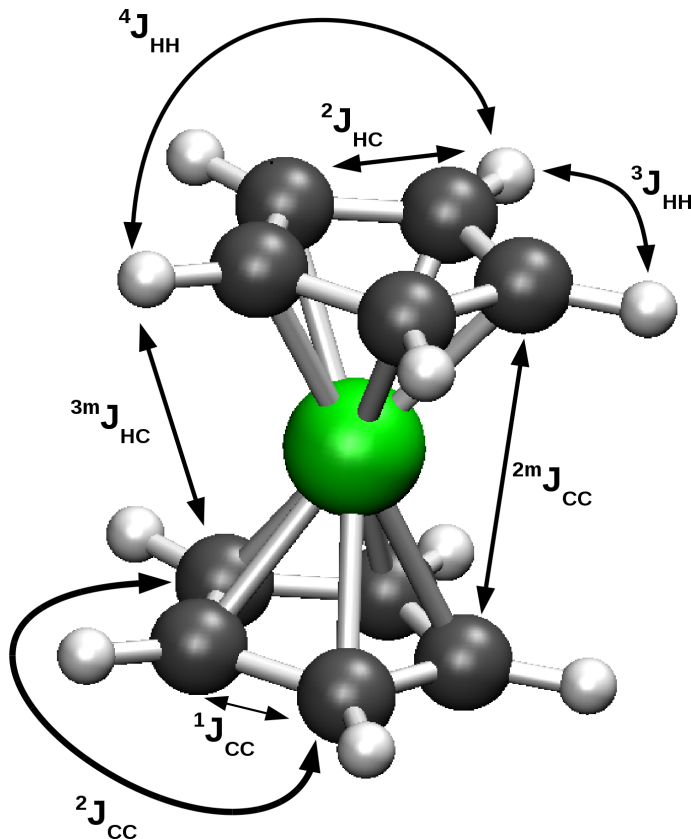

Figure 1: Metallocene structure with some of the possible spin-spin couplings labeled. Carbon atoms are in grey, hydrogens in white, and the metal center in green.

Both $NiCp_2$ and $CrCp_2$ have a triplet ($S = 1$) ground state and, effectively, a 5-fold axial symmetry as a result of intramolecular dynamics. However, at the B3LYP optimized equilibrium geometry, the rotational symmetry is not perfectly preserved, and the individual CC and CX (X=Ni or Cr) bond lengths of the optimized geometry vary by circa 0.03 Å around the cyclopentadienyl ring. To determine whether this variability has significant impact on the paramagnetic enhancements $\mathbf{J}^p_{KL}$, the latter were also calculated for perfectly symmetrized structures of nickelocene, with the bond lengths fixed at the average bond lengths of the B3LYP-optimized geometry. The effect of symmetrizing the structures was found to be small, and shall not be discussed further. The results

for the symmetrized structure are deposited in Table S1 of the SI.

Under experimental conditions the cyclopentadienyl rings of the metallocenes (Fig. 1) can be expected to rotate independently from one another about the axis of symmetry of the molecule. Consequently, couplings between pairs of nuclei on different rings can not be distinguished by the relative position of the nuclei within the two rings. In light of this, all results obtained in this paper are reported by averaging over all such indistinguishable pairs of nuclei, *e.g.*, only one inter-ring coupling enhancement of each type (CC, CH, HH), is given.

As implied above, the rotation of the cyclopentadienyl rings renders these metallocenes effectively cylindrically symmetric from the experimental point of view. Therefore, all tables reporting results for the metallocenes only list the isotropic enhancement, J_{iso}^p, as well as the anisotropy ΔJ^p with respect to the axis of cylindrical symmetry (in this case the z-axis). The paramagnetic contributions to SSCC and the coupling anisotropy are defined by

$$J_{\text{iso}}^p = \frac{\text{Tr}(\mathbf{J}^p)}{3} \; ; \qquad \Delta J^p = J_{zz} - \frac{J_{xx} + J_{yy}}{2}. \tag{10}$$

We assume that the experimental conditions, which cover a range of inter- and intramolecular dynamics, are adequately approximated by the present average over equivalent couplings in the static, optimised equilibrium geometry. The resulting errors are likely to be insignificant for the purpose of this paper, which is to introduce and give rough estimates for the size of $\mathbf{J}^p$.

The magnitude of the enhancement mainly depends on three factors. The first is constituted by the strengths of the nuclear magnetic moments. Secondly, electronic properties — in the NR realm the spin density at the site of the nucleus — are affected by the distance from the paramagnetic centre. Together these two factors determine the magnitude of the HFC. The third factor is the orientation of the principal axes of the HFC tensors of the two nuclei with respect to those of the $\langle \mathbf{SS} \rangle$ dyadic, the latter determined by the ZFS tensor.

Table 2 lists the results for the paramagnetic enhancements for the two paramagnetic metallocenes, as well as the conventional SSCCs of diamagnetic FeCp$_2$. Table S2 in the SI reports the

12

Table 2: Computed isotropic paramagnetic enhancement, J^p_{KL}, of spin-spin coupling constants of metallocenes $NiCp_2$ and $CrCp_2$ compared to the unenhanced, standard coupling constants, J_{KL}, in the diamagnetic $FeCp_2$. All values in Hz. [a]

| Coupling | Enhancement J^p | | Standard J |
	$NiCp_2$	$CrCp_2$	$FeCp_2$
$^3J_{HH}$	0.65	1.50	8.0
$^4J_{HH}$	0.82	1.17	-0.1
$^1J_{CC}$	5.42	-0.02	88.5
$^2J_{CC}$	5.63	-0.17	-4.1
$^1J_{CH}$	-1.17	-0.04	172.9
$^2J_{CH}$	-1.79	-0.51	3.8
$^3J_{CH}$	-1.90	-0.74	3.8
$^{4m}J_{HH}$	1.24	1.79	0.0
$^{2m}J_{CC}$	5.66	0.11	-0.3
$^{3m}J_{CH}$	-1.66	-0.48	0.0

[a] With HFCs calculated using the fully relativistic RESPECT-MDKS method.

corresponding components of the **A** tensor along and perpendicular to the molecular symmetry axis. For $NiCp_2$, the order of magnitude of the SSCC enhancements is CC > CH > HH, which is what would be expected based on the first two of the three principles laid out above. For example, the CC results for $NiCp_2$ demonstrate the significance of the paramagnetic enhancement; particularly the magnitude of $^{2m}J^p_{CC}$ is far greater than that of the unenhanced coupling $^{2m}J_{CC}$ calculated for $FeCp_2$. Significant enhancements are also seen for the $^{4m}J^p_{HH}$ and $^{3m}J^p_{CH}$ results.

The coupling enhancements in $CrCp_2$ are much smaller than in $NiCp_2$ and, intriguingly, the HH couplings are more strongly enhanced than the CC couplings. A possible reason for this is that the spin density is more localized on the metal center in $CrCp_2$ than it is in $NiCp_2$, resulting in a smaller hyperfine shielding of the carbons.[13,21] Accordingly, in $CrCp_2$, the main cause of the proton and carbon HFCs is the spin polarization of the molecular orbitals near these nuclei[4] (as mentioned earlier, all the present DFT calculations were unrestricted).

Tables 3 and 4 compare the SSC enhancements, J^p and ΔJ^p, obtained with the HFC tensors calculated using a fully relativistic matrix-Dirac-Kohn-Sham method, in which the SO coupling effects are included variationally, with those obtained from the HFC tensors calculated using NR

theory augmented by a perturbational SO correction. In these 3d systems the *J*-enhancements are not significantly affected by the choice between the two methods; differences are a couple of Hz at most. The choice between the methods of obtaining the HFCs is not equally crucial to $\mathbf{J}^p$ as it is for the corresponding hyperfine shieldings, where using fully relativistic HFCs generally improves the agreement with experiment.

Table 3: Comparison of the paramagnetic spin-spin coupling enhancement, $\mathbf{J}^p$, for nickelocene, calculated using HFC tensors obtained from the spin-orbit corrected nonrelativistic (NR+SO) and fully relativistic 4-component (DKS) methods. Results for both the enhancement of the isotropic coupling constant (J_{iso}^p) and the coupling anisotropy (ΔJ^p) are shown. All values in Hz. [a]

	J_{iso}^p		ΔJ^p	
Coupling	NR+SO	DKS	NR+SO	DKS
$^3J_{\text{HH}}$	0.63	0.65	1.38	0.48
$^4J_{\text{HH}}$	1.18	0.82	-1.42	-0.38
$^1J_{\text{CC}}$	5.53	5.42	16.05	16.43
$^2J_{\text{CC}}$	4.81	5.63	15.29	16.63
$^1J_{\text{CH}}$	-0.81	-1.17	-3.59	-3.58
$^2J_{\text{CH}}$	-1.60	-1.79	-3.59	-3.66
$^3J_{\text{CH}}$	-2.18	-1.90	-4.63	-4.01
$^{4m}J_{\text{HH}}$	1.38	1.24	-0.29	-0.42
$^{2m}J_{\text{CC}}$	5.35	5.66	15.82	16.62
$^{3m}J_{\text{CH}}$	-1.76	-1.66	-4.16	-3.79

[a] The HFC tensors were calculated using DFT (PBE0) as described in the text. Anisotropies are defined with respect to the axis of cylindrical symmetry.

Consideration of the enhancements of some specific couplings can help to provide a qualitative feeling for the mechanisms by which the enhancement works. Table 5 and the SI Table S3, show that the isotropic components of $^3\mathbf{J}_{\text{HH}}^p$ and $^4\mathbf{J}_{\text{HH}}^p$, respectively, are dominated by the J_{con}^p and J_{dip}^p contributions (see Table 1), whilst the anisotropic term is dominated by J_{dip}^p, with some significance of the $J_{\text{con-dip}}^p$ term, too. This pattern is observed in several of the metallocene couplings, and can be analyzed in terms of the symmetry of the molecule and expressions in Table 1. The J_{con}^p term arises from ZFS and the leading-order isotropic HFC constants. However, due to the near-symmetry of the ring in the optimized geometry, the electron spin density mediates all couplings in the plane of the ring with similar efficiency. Furthermore, due to the symmetry, the HFC tensors

Table 4: As Table 3 but for chromocene.

Coupling	J^p_{iso}		ΔJ^p	
	NR+SO	DKS	NR+SO	DKS
$^3J_{\text{HH}}$	2.23	1.50	1.63	1.20
$^4J_{\text{HH}}$	0.72	1.17	-0.02	0.41
$^1J_{\text{CC}}$	0.31	-0.02	0.53	-0.11
$^2J_{\text{CC}}$	-0.29	-0.17	-0.62	-0.44
$^1J_{\text{CH}}$	0.11	-0.04	-0.19	0.06
$^2J_{\text{CH}}$	-0.48	-0.51	-0.19	-0.11
$^3J_{\text{CH}}$	-0.98	-0.74	-0.86	-0.68
$^{4m}J_{\text{HH}}$	2.01	1.79	0.87	0.80
$^{2m}J_{\text{CC}}$	0.16	0.11	0.19	0.08
$^{3m}J_{\text{CH}}$	-0.68	-0.48	-0.58	-0.31

of any two protons in the ring have roughly equivalent isotropic parts, hence the magnitude of the associated contributions to the coupling enhancement will also be roughly equivalent for all proton pairs in the ring.

The decomposition of $^1\mathbf{J}^p_{\text{CC}}$ (Table S4 in the SI again highlights the significance of the J^p_{con} and J^p_{dip} terms. However, unlike for $^4\mathbf{J}^p_{\text{HH}}$, the $J^p_{\text{con-dip}}$ term is found to dominate the anisotropy, ΔJ^p, of the enhancement. This is a consequence of the increase in the Fermi-contact contribution to the ^{13}C HFC tensors when compared to the protons. For the enhancement of the $^2\mathbf{J}_{\text{CC}}$ coupling (Table S5 in SI), we observe a pattern of contributions similar to that in $^1\mathbf{J}^p_{\text{CC}}$. This can again be attributed to the roughly cylindrically symmetric spin density. The relative magnitude of the $\mathbf{J}^p_{\text{dip}}$ term is determined by the relative orientations of the principal axes of the pertinent HFC tensors.

A distinguishing feature of the coupling enhancement is its lack of a direct dependence on the number of bonds separating the two coupled nuclei. This is illustrated by the intra-ring CH couplings in NiCp$_2$ and CrCp$_2$ (Table 2), where the isotropic enhancement actually *increases* in magnitude as the coupled nuclei become further apart, *i.e.*, $|^3J^p_{\text{CH}}| > |^2J^p_{\text{CH}}| > |^1J^p_{\text{CH}}|$. It is worth noting that due to the symmetry of the ring the physical contributions to all these couplings (Table 6 here, as well as the SI Tables S6 and S7) arising from the (isotropic) contact HFC are equivalent, *i.e.*, $^1J^p_{\text{CH,con}} = {}^2J^p_{\text{CH,con}} = {}^3J^p_{\text{CH,con}}$. The difference between the magnitudes of the 1-, 2- and 3-bond couplings arises purely from the dipolar contribution, $\mathbf{J}^p_{\text{dip}}$, and the associated difference

in the orientation of the principal axes of the HFC tensors of the coupled hydrogen and carbon nuclei. The reason this pattern is not observed in $CrCp_2$ is probably that, whilst $NiCp_2$ largely retained its symmetric geometry following the optimization, the $CrCp_2$ geometry was distorted more significantly. Tables S8–S11 in the SI contain the analyses of further coupling enhancement terms in the present two metallocenes.

An interesting consequence of the independence of the coupling enhancements from the inter-nuclear separation distance is that even if the paramagnetic enhancements can be quite small at close range (as compared to the normal diamagnetic coupling), they can become relatively significant for well-separated nuclei. From Table 2 it is clear that for the intra-ring couplings $J^p \lesssim J$, but that for couplings between the rings this relationship is mostly reversed: $^m J^p \gtrsim {}^m J$. In fact, the two kinds of coupling enhancement tensors differ mainly in one respect; the difference mainly arises from the sign reversal of the zz component (along the molecular axis) of the first-order SO contribution to the HFC tensors, which is a consequence of the plane of mirror symmetry between the two cyclopentadienyl rings.

The distance-independent behavior indicates that spin-spin coupling in paramagnetic systems represents a qualitatively distinct addition to the standard spin-spin coupling. Furthermore, it suggests that, particularly when long-range couplings are considered, the SSCCs for diamagnetic systems may not always constitute a good approximation to the SSCCs of similar paramagnetic molecules. One can foresee that, in certain cases of also short-range, *e.g.*, two-bond (geminal) couplings, the paramagnetic enhancements can exceed the magnitude of the conventional coupling mechanisms.

$Cr(acac)_2$ complex

The coupling enhancements were also calculated for a Cr(II) acetyl-acetatonate complex, $Cr(acac)_2$ (Fig. 2). This complex was chosen because similar systems are known to exhibit significant ZFS.[43] In this system the H and C nuclei are relatively far from the paramagnetic center, indicating that the couplings between them may be easier to measure experimentally than in the metallocenes, how-

Table 5: Contributions to $^3\mathbf{J}^p_{\mathrm{HH}}$ for nickelocene and chromocene. The HFC tensors used to calculate the enhancements were obtained using the SO-corrected NR method. All values in Hz.

Contribution	J^p_{iso}		ΔJ^p	
	NiCp$_2$	CrCp$_2$	NiCp$_2$	CrCp$_2$
J^p_{con}	1.36	2.02	-0.13	0.05
$J^p_{\mathrm{con-dip}}$	0.00	0.00	-0.11	0.73
J^p_{dip}	-0.72	0.19	1.57	0.88
$J^p_{\mathrm{con-pc}}$	0.02	0.01	0.00	0.00
$J^p_{\mathrm{con-dip2}}$	0.00	0.00	-0.04	0.00
$J^p_{\mathrm{con-as}}$	—	—	0.00	0.00
$J^p_{\mathrm{dip-pc}}$	0.00	0.00	0.00	0.00
$J^p_{\mathrm{dip-dip2}}$	-0.03	0.01	0.08	0.00
$J^p_{\mathrm{dip-as}}$	0.00	0.00	0.03	-0.03
J^p_{total}	0.63	2.23	1.38	1.63

Table 6: As Table 5 but for $^1\mathbf{J}^p_{\mathrm{CH}}$.

Contribution	J^p_{iso}		ΔJ^p	
	NiCp$_2$	CrCp$_2$	NiCp$_2$	CrCp$_2$
J^p_{con}	-1.87	-0.74	0.18	-0.02
$J^p_{\mathrm{con-dip}}$	0.09	0.00	-4.18	-0.56
J^p_{dip}	0.84	0.84	0.38	0.38
$J^p_{\mathrm{con-pc}}$	0.04	0.04	0.00	0.00
$J^p_{\mathrm{con-dip2}}$	0.00	0.00	-0.05	0.01
$J^p_{\mathrm{con-as}}$	—	—	0.00	0.00
$J^p_{\mathrm{dip-pc}}$	0.00	0.00	-0.04	0.01
$J^p_{\mathrm{dip-dip2}}$	0.08	-0.02	0.04	0.00
$J^p_{\mathrm{dip-as}}$	0.00	0.00	0.08	-0.01
J^p_{total}	-0.81	0.11	-3.59	-0.19

ever, the paramagnetic enhancements of all CH couplings were found to be very small (Table 7). The strongest enhancement of HH couplings was found in the CH_3 ligands, $^2\mathbf{J}_{HH}$, which averaged to ~0.2 Hz. Larger enhancements of around ~2 Hz were calculated for CC couplings (Table 7). Somewhat more pronounced coupling enhancements were obtained for the OO couplings (~4 Hz), however, SSCCs between two ^{17}O are notoriously difficult to obtain experimentally, even in diamagnetic systems.

The enhancement of CH couplings was in this case smaller due to the localization of the spin density at the paramagnetic center, causing only modest HFC of nuclei not directly bonded to the metal ion. A noteworthy feature of these results is that the enhancement of, *e.g.*, the couplings between carbon nuclei on the opposite sides of the complex are practically identical to the couplings of equivalent pairs of nuclei on the same ligand, *e.g.*, $^{5m}J^p_{CC} \approx ^1 J^p_{CC}$. This is a consequence of the distance-independence of the paramagnetic enhancement, and the fact that the HFC arises in this case mainly due to the isotropic Fermi contact term, and not the dipolar term. This reduces the significance of the orientation of the principal axes of the two relevant HFC tensors to the coupling enhancement.

Table 7: Selected paramagnetic spin-spin coupling enhancements for $Cr(acac)_2$ complex. All values in Hz. See Fig. 2 for the coupling notation. The J^p_i $(i = 1, 2, 3)$ denote the principal axes of the coupling enhancement tensor. The coupling tensors were calculated using the fully relativistic RESPECT-MDKS method.

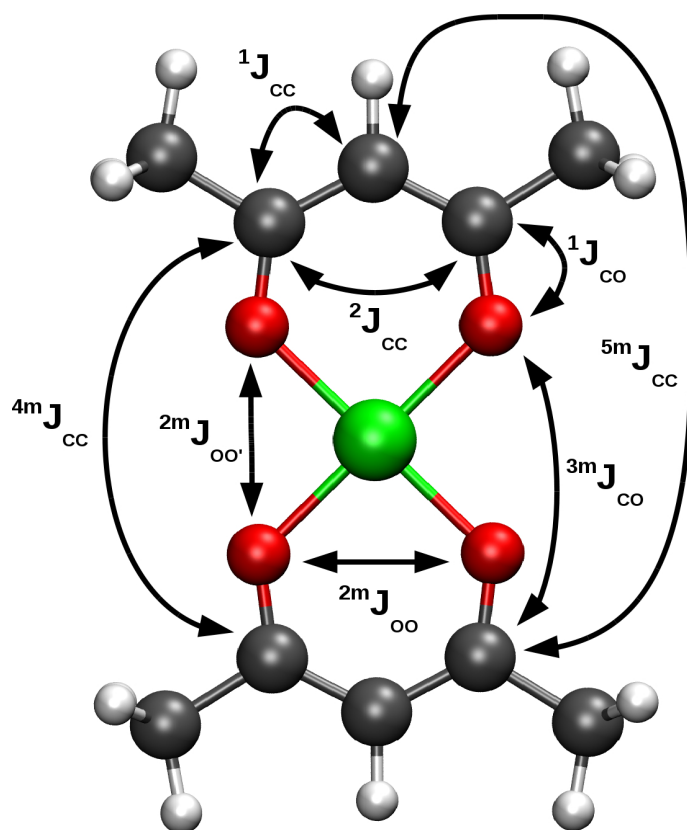| Coupling	J^p_1	J^p_2	J^p_3	J^p_{iso}
$^{2m}J_{OO}$	2.35	3.14	5.37	3.62
$^{2m}J_{OO'}$	2.35	3.14	5.37	3.62
$^1J_{CO}$	0.92	2.87	4.09	2.63
$^{3m}J_{CO}$	0.92	2.87	4.09	2.63
$^2J_{CC}$	0.33	2.35	3.11	1.93
$^{4m}J_{CC}$	0.33	2.35	3.11	1.93
$^1J_{CC}$	-0.21	-0.14	1.14	0.26
$^{5m}J_{CC}$	-0.21	-0.14	1.14	0.26

Figure 2: Chromium di-acetylacetatonate [Cr(acac)$_2$] complex with significant couplings labeled, the central Cr atom in green.

Table 8: Computed paramagnetic enhancement, J^p_{iso} of the isotropic ^{1}H^{1}H spin-spin coupling constants for a Co(II) pyrazolylborate complex (HPYBCO). The numbering of atoms refers to Fig. 3. For the notation of the couplings see.[44] Several couplings are equivalent, and have been averaged over to obtain the results in the Table. The HFC tensors used in determination of these couplings were obtained using RESPECT-MDKS. All values in Hz.

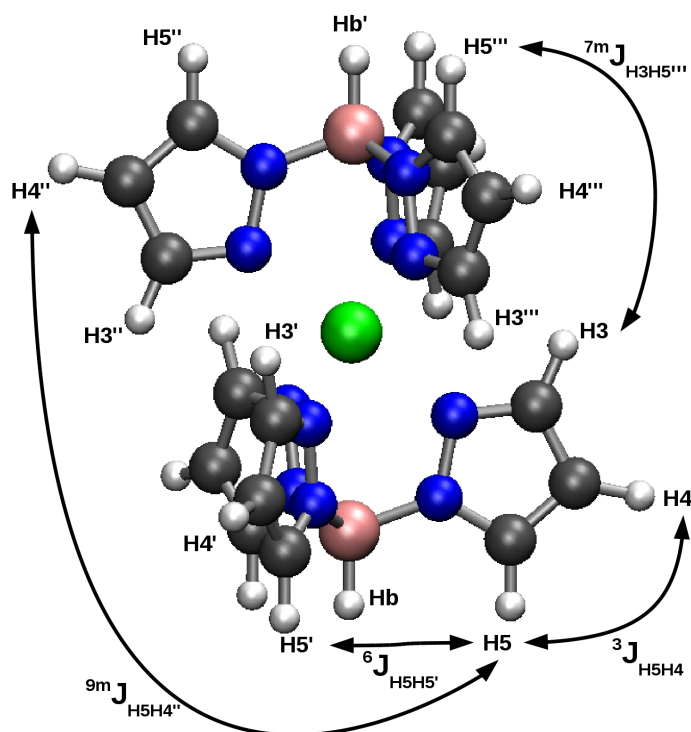| Coupling	J^p_{iso}	Coupling	J^p_{iso}
$^3J_{\text{H5H4}}$	0.10	$^9J_{\text{H5H4}''}$	0.10
$^4J_{\text{H5H3}}$	-0.08	$^7J_{\text{H5H3}''}$	-0.08
$^4J_{\text{H5Hb}}$	0.19	$^8J_{\text{H5Hb}''}$	0.19
$^3J_{\text{H4H3}}$	0.23	$^7J_{\text{H4H3}''}$	0.23
$^5J_{\text{H4Hb}}$	-0.02	$^8J_{\text{H4Hb}''}$	-0.02
$^6J_{\text{H3Hb}}$	-0.41	$^7J_{\text{H3Hb}''}$	-0.41
$^8J_{\text{HbHb}}$	-0.40	$^8J_{\text{H5H5}''}$	0.19
————	——	$^8J_{\text{H4H4}''}$	0.12
————	——	$^6J_{\text{H3H3}''}$	1.28
$^6J_{\text{H5H5}'}$	0.05	$^8J_{\text{H5H5}'''}$	0.05
$^8J_{\text{H4H4}'}$	-0.04	$^8J_{\text{H4H4}'''}$	-0.04
$^{10}J_{\text{H3H3}'}$	-0.03	$^6J_{\text{H3H3}'''}$	-0.03
$^7J_{\text{H5H4}'}$	-0.04	$^9J_{\text{H5H4}'''}$	-0.04
$^8J_{\text{H5H3}'}$	-0.23	$^7J_{\text{H5H3}'''}$	-0.23
$^9J_{\text{H4H3}'}$	-0.08	$^7J_{\text{H4H3}'''}$	-0.08

Figure 3: Co(II) pyrazolylborate complex (HPYBCO) with labeling of some of the possible HH spin-spin couplings. The structure has D_{3d} symmetry. This diagram covers all the experimentally distinguishable cases of couplings between different rings. The notation for the inter-ring couplings is $^{n}J_{HiHj}$, whilst $^{n}J_{HiHj'}$, $^{n}J_{HiHj''}$, and $^{n}J_{HiHj'''}$ denote the different experimentally distinguishable inter-ring couplings. For the notation see.[44]

Co(II) pyrazolyl borate complex

The paramagnetic SSC enhancement was calculated for the Co(II) (HPYBCO) complex (Fig. 3). This complex has been investigated earlier in Refs.,[13,21] where significant paramagnetic enhancements to the ^{1}H shielding constants were observed. As this shielding enhancement is formally analogous to the present SSC enhancement, a strong enhancement of the J_{HH} could be expected. However, the paramagnetic enhancements for this system turn out to again be relatively low (see Table 8), with the isotropic contribution, J^p_{iso}, consistently below 2 Hz. Significant paramagnetic effects on shieldings do not, as seen here, necessarily imply major effects on couplings.

Gd-DOTA complex

The coupling enhancements in Gd-DOTA (Fig. 4), a gadolinium(III)-based MRI contrast agent, were also investigated. Part of the reason for choosing this complex is its high multiplicity ($2S + 1 = 8$). As noted above, the trace of the $\langle S_a S_b \rangle$ dyadic is approximately equal to S^2 and, therefore, the expected overall paramagnetic enhancement scales with the multiplicity. Furthermore, the heavy lanthanide center means that significant relativistic effects are expected. The first prediction is confirmed by the relatively large HH coupling enhancements, up to circa 6.6 and 9.4 Hz for the isotropic coupling constant, and anisotropy, respectively, included in Table 9. It is worth mentioning that Gd-DOTA was found to have a very small ZFS, with the computed $D \approx -0.068\ \text{cm}^{-1}$ at the NEVPT2 level. Therefore, the anisotropy of the SSC enhancement stems almost entirely from the relative anisotropy of the HFC tensors of the two coupled nuclei. The Gd-DOTA complex provides a clear illustration of the paramagnetic enhancement being independent of the relative location of the nuclei in the molecule; the largest isotropic coupling enhancement found here is between two protons separated by five bonds.

It is interesting to note that a fully variational treatment of both scalar relativistic effects and SO coupling using the RESPECT-MDKS code was not found to be necessary from the qualitative point of view. This is somewhat surprising considering that relativistic effects are normally found highly significant for lanthanide-based compounds. In general, relativistic effects on the pNMR

properties of protons are of somewhat lesser importance than for ^{13}C, and they also diminish with the distance of the nucleus from the heavy-atom center. The ZFS tensor was calculated at the 2nd-order DKH level that, due to the comparatively small scalar relativistic influences on this quantity, should constitute an adequate approximation. It should be noted that the similarity of the ORCA and RESPECT-MDKS results can in part also be a consequence of using a relatively modest basis set in the present pilot study.

Table 9: Comparison of the paramagnetic spin-spin coupling enhancements, $\mathbf{J}^p$, for selected HH spin-spin couplings in Gd-DOTA, calculated using HFC tensors obtained from the spin-orbit corrected nonrelativistic (NR+SO) and fully relativistic 4-component (DKS) methods. The anisotropy was taken with respect to the axis of rotation. All values in Hz, only enhancements above 2 Hz included. See Fig. 4 for a clarification of the coupling notation.

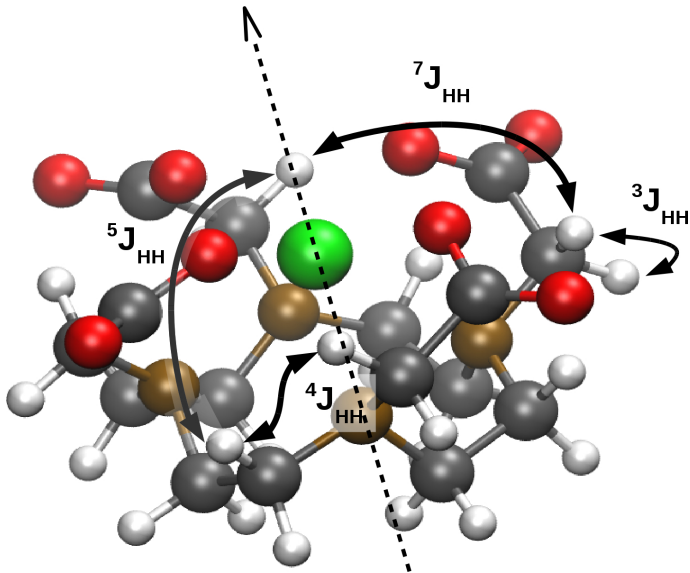| Coupling | J^p_{iso} | | ΔJ^p | |
	NR+SO	DKS	NR+SO	DKS
$^3J_{HH}$	2.40	2.40	-1.79	-1.35
$^4J_{HH}$	2.53	2.58	-1.99	-1.99
$^5J_{HH}$	6.52	6.59	-5.41	-5.40
$^7J_{HH}$	-3.22	-3.27	9.21	9.41

Figure 4: Gd-DOTA complex with relevant spin-spin couplings labeled. The nitrogen atoms in bronze and the Gd atom in green. The axis of rotational symmetry of the complex is represented by the dotted line.

Conclusions

The spin-spin coupling tensor in paramagnetic molecules is subject to a paramagnetic enhancement. This enhancement may, to a reasonable approximation, be determined from the HFC and ZFS tensors. The size of the enhancement is found to vary significantly between systems, and to be dependent on the spin multiplicity, the magnitude of hyperfine coupling, and the anisotropy of the ZFS and HFC tensors. The enhancement is shown to be significant in the CC, CH, and HH couplings in 3d metallocenes and the lanthanide complex Gd-DOTA, but small in the HH couplings of a Cr(II) acetyl-acetatonate compound, and almost negligible in a Co(II) pyrazolylborate complex. Whilst fully relativistic mDKS calculations were found to be unnecessary for the systems included in this study, it is likely that a more in-depth study could reveal their importance, particularly for couplings between NMR nuclei heavier than a proton and/or located close to the heavy paramagnetic center. The qualitative features of the enhancement are captured already in nonrelativistic calculations, however.

An interesting property of the paramagnetic enhancement is that its magnitude has no direct dependence upon the distance between the two coupled nuclei. Consequently, as the separation of the two coupled nuclei increases, so does the importance of the paramagnetic enhancement relative to the corresponding diamagnetic coupling. This was demonstrated, *e.g.*, by the result that the paramagnetic enhancement to the SSCC between two carbon nuclei on the different cyclopentadienyl rings of $NiCp_2$ is in fact larger than the corresponding (unenhanced) SSCC in the diamagnetic $FeCp_2$. This suggests that approximating the SSCCs of a paramagnetic system with those of the corresponding diamagnetic molecule may not always be valid. Hence, qualitatively the *J*-coupling enhancement is an indirect phenomenon where two nuclei are individually coupled to the electron spin distribution, and the magnitude of the effect is influenced by the relative positions of the nuclei with respect to the paramagnetic center. With the development of experimental pNMR procedures, the paramagnetic spin-spin coupling enhancement is highly likely to become significant.

Acknowledgement

Supporting Information Available

Derivation of the paramagnetic enhancement of spin-spin coupling; the optimized geometries of $FeCp_2$ and $Cr(acac)_2$, comparison of the calculated coupling enhancements of the symmetrized and as-optimized eclipsed structures of $NiCp_2$, the components of the ^{13}C and ^1H HFC tensors of $NiCp_2$ and $CrCp_2$, as well as tabulated break-down of the enhancements of various couplings in the two studied metallocenes.

This material is available free of charge via the Internet at `http://pubs.acs.org/`.

References

(1) Krivdin, L. B.; Kalabin, G. A. *Progr. NMR Spectrosc.* **1989**, *21*, 293.

(2) Bertini, I.; Turano, P.; Vila, A. J. *Chem. Rev.* **1993**, *93*, 2833.

(3) Bertini, I.; Emsley, L.; Lelli, M.; Luchinat, C.; Mao, J.; Pintacuda, G. *J. Am. Chem. Soc.* **2010**, *132*, 5558.

(4) Bertini, I.; Luchinat, C. *Coord. Chem. Rev.* **1999**, *150*, 1.

(5) Bertini, I.; Luchinat, C.; Parigi, G.; Pierattelli, R. *Dalton Transactions* **2008**, *29*, 3782.

(6) Güntert, P.; Wüthrich, K. *J. Biomol. NMR* **1991**, *1*, 447.

(7) Bose-Basu, B.; Klepach, T.; Bondo, G.; Bondo, P. B.; Zhang, W.; Carmichael, I.; Serianni, A. S. *J. Org. Chem.* **2007**, *72*, 7511.

(8) Zhuang, T. *Prot. Sci.* **2008**, *17*, 1220.

(9) Kowalewski, J.; Mäler, L. *Nuclear Spin Relaxation in Liquids: Theory, Experiments, Applications* (CRC Press, Boca Raton, 2006).

(10) Benda, L.; Mareš, J.; Ravera, E.; Parigi, G.; Luchinat, C.; Kaupp, M.; Vaara, J. *Angew. Chem., Int. Ed.* **2016**, *55*, 14713.

(11) Autschbach, J. *Ann. Rep. Comput. Chem.* **2015**, *11*, 3.

(12) Kurland, R. J.; McGarvey, B. R. *J. Magn. Reson.* **1970**, *2*, 286.

(13) Vaara, J.; Rouf, S. A.; Mareš, J. *J. Chem. Theory Comput.* **2015**, *11*, 4840.

(14) Van den Heuvel, W.; Soncini, A. *Phys. Rev. Lett.* **2012**, *109*, 073001.

(15) Van den Heuvel, W.; Soncini, A. *J. Chem. Phys.* **2013**, *138*, 054113.

(16) Pennanen, T. O.; Vaara, J. *J. Chem. Phys.* **2005**, *123*, 133002.

(17) Arbuznikov, A. V.; Vaara, J.; Kaupp, M. *J. Chem. Phys.* **2004**, *120*, 2127.

(18) Autschbach, J.; Patchkovskii, S.; Pritchard, B. *J. Chem. Theory Comput.* **2011**, *7*, 2175.

(19) Komorovsky, S.; Repisky, M.; Ruud, K.; Malkina, O. L.; Malkin, V. G. *J. Phys. Chem.* **2013**, *117*, 14209.

(20) Komorovský, S.; Repiský, M.; Malkina, O. L.; Malkin, V. G.;Ondík, I. M.; Kaupp, M. *J. Chem. Phys.* **2008**, *128*, 104101.

(21) Rouf, S. A.; Mareš, J.; Vaara, J. *J. Chem. Theory Comput.* **2015**, *11*, 1683.

(22) TURBOMOLE V6.5 2013, a development of University of Karlsruhe Forschungszentrum Karlsruhe GmbH, TURBOMOLE GmbH: 1989–2007. Available from http://www.turbomole.com.

(23) Lee, C.; Yang, W.; Parr, R. G. *Phys. Rev. B* **1988**, *37*, 785; Becke, A. D. *J. Chem. Phys.* **1993**, *98*, 5648; Stephens, P. J.; Devlin, F. J.; Chabalowski, C. F.; Frisch, M. J. *J. Phys. Chem.* **1994**, *98*, 11623.

(24) Weigend, F.; Ahlrichs, R. *Phys. Chem. Chem. Phys.* **2005**, *7*, 3297; *Ibid.* **2006**, *8*, 1057.

(25) Dolg, M.; Wedig, U.; Stoll, H.; Preuss, H. *J. Chem. Phys.* **1987**, *86*, 866.

(26) Martin, J. M. L.; Sundermann, A. *J. Chem. Phys.* **2001**, *114*, 3408.

(27) Neese, F. ORCA, *An ab Initio, Density Functional and Semiempirical Program Package*, Version 3.0.1 **2012**.

(28) Grimme, S. *J. Comput. Chem.* **2006**, *27*, 1787.

(29) Schaefer, A.; Horn, H.; Ahlrichs, R. *J. Chem. Phys.* **1992**, *97*, 2571.

(30) Angeli, C.; Cimiraglia, R.; Evangelisti, S.; Leininger, T.; Malrieu, J. P. *J. Chem. Phys.* **2001**, *114*, 10252; Angeli, C.; Cimiraglia, R.; Malrieu, J. P.; *Chem. Phys. Lett.* **2001**, *350*, 297; Angeli, C.; Cimiraglia, R.; Malrieu, J. P. *J. Chem. Phys.* **2002**, *117*, 9138; Angeli, C.; Borini, S.; Cimiraglia, R. *Theor. Chem. Acc.* **2004**, *111*, 352.

(31) Pantazis, D. A.; Chen, X. Y.; Landis, C. R.; Neese, F. *J. Chem. Theory Comput.* **2008**, *4*, 908.

(32) Douglas, M.; Kroll, N. M. *Ann. Phys.* **1974**, *82*, 89.

(33) Jansen, G.; Hess, B. A. *Phys. Rev. A* **1989**, *39*, 6016.

(34) Chesnut, D. B.; Moore, J. *J. Comput. Chem.* **1989**, *10*, 648; Jensen, J. H.; Gordon, S. M. *J. Comput. Chem.* **1991**, *12*, 42; DiLabio, A. G.; Pratt, D. A.; LoFaro, A. D.; Wright, J. S. *J. Phys. Chem.* **1999**, *103*, 1653.

(35) McNamara, J. P.; Berrigan, S. D.; Hillier, I. H. *J. Chem. Theory Comput.* **2007**, *3*, 1014.

(36) Repiský, M.; Komorovský, S.; Malkin, V. G.; Malkina, O. L.; Kaupp, M.; Ruud, K.; Bast, R.; Ekström, U.; Knecht, S.; Malkin, O. I.; Malkin, E. Relativistic Spectroscopy DFT program, Version 3.3.0 (beta) **2013**.

(37) Perdew, J. P.; Burke, K.; Ernzerhof, M. *Phys. Rev. Lett.* **1996**, *77*, 3865; **1997**, *78*, 1396(E).

(38) Adamo, C.; Barone, V. *J. Chem. Phys.* **1999**, *110*, 6158.

(39) Frisch, M. J. *et al.* Gaussian 09, Revision D.01 (Gaussian, Inc.: Wallingford, CT, 2009).

(40) Malkin, E.; Repiský, M.; Komorovský, S.; Mach, P.; Malkina, O. L.; Malkin, V. G. *Phys. Chem. Chem. Phys.* **2011**, *134*, 044111.

(41) Neese, F. *J. Chem. Phys.* **2003**, *118*, 3939; Neese, F. *J. Chem. Phys.* **2005**, *122*, 034107; Neese, F. *J. Chem. Phys.* **2007**, *127*, 164112.

(42) Hrobárik, P.; Reviakine, R.; Arbuznikov, A. V.; Malkina, O. L.; Malkin, V. G.; Köhler, F. H.; Kaupp, M. *J. Chem. Phys.* **2007**, *126*, 024107.

(43) Miller, J.; Schaefle, N.; Sharp, R. *Magn. Reson. Chem.* **2003**, *41*, 806.

(44) $^{3}J^{p}_{\text{H5H4}}$ denotes the enhancement of the coupling between hydrogens H5 and H4 located on the same ring. $^{6}J^{p}_{\text{H5H5}'}$ is the enhancement of the coupling between hydrogens H5 and H5', nuclei that are on separate rings, which, however, are both on the same side of the horizontal plane of symmetry perpendicular to the principal axis of rotation. $^{7}J^{p}_{\text{H5H3}''}$ is the enhancement of the coupling between hydrogens H5 and H3$''$, which are on separate rings opposite (*trans*) to one another, on different sides of the plane of symmetry perpendicular to the principal axis. Finally, $^{7}J^{p}_{\text{H3H5}'''}$ is the enhancement of the coupling between hydrogens H3 and H5$'''$, which are on separate rings that are not opposite to one another, and which are on different sides of the horizontal plane. The left superscript is the number of chemical bonds which separate the two nuclei.

Graphical TOC Entry